

PAPER • OPEN ACCESS

# Grinding characteristics during ultrasonic vibration assisted grinding of alumina ceramic in selected dry and MQL conditions

Recent citations

- [Design and development of an ultrasonic stack assembly for ultrasonic vibration assisted grinding](#)  
Sreethul Das *et al*

To cite this article: Sreethul Das and C Pandivelan 2020 *Mater. Res. Express* 7 085404

View the [article online](#) for updates and enhancements.



The Electrochemical Society  
Advancing solid state & electrochemical science & technology  
2021 Virtual Education

**Fundamentals of Electrochemistry:**  
Basic Theory and Kinetic Methods  
Instructed by: **Dr. James Noël**  
Sun, Sept 19 & Mon, Sept 20 at 12h–15h ET

Register early and save!





## PAPER

## Grinding characteristics during ultrasonic vibration assisted grinding of alumina ceramic in selected dry and MQL conditions

## OPEN ACCESS

RECEIVED  
4 May 2020REVISED  
26 July 2020ACCEPTED FOR PUBLICATION  
6 August 2020PUBLISHED  
19 August 2020Sreethul Das  and C Pandivelan 

School of Mechanical Engineering, Vellore Institute of Technology, Vellore, Tamil Nadu, India

E-mail: [cpandivelan@vit.ac.in](mailto:cpandivelan@vit.ac.in)**Keywords:** ultrasonic assisted grinding, ceramics, Grey relational analysis, 3D parameters, surface quality, dry and MQL conditions

Original content from this work may be used under the terms of the [Creative Commons Attribution 4.0 licence](https://creativecommons.org/licenses/by/4.0/).

Any further distribution of this work must maintain attribution to the author(s) and the title of the work, journal citation and DOI.

**Abstract**

Ultrasonic vibration assisted grinding (UAG) has proven to lower the forces and improve the ground surface quality while shaping difficult to grind materials such as ceramics. A systematic study of UAG of alumina ceramic using a metal bonded diamond grinding wheel has been performed here. Taguchi's L18 array based experimentation has been performed to study the effect of UAG parameters. During UAG, the vibration amplitudes of 6 and 12 microns have been used and the frequency has been kept at 20 kHz. From these experiments, optimum parameters for UAG have been identified using Grey relational analysis. Mathematical models generated using regression analysis have been found to correlate the experimental data with good accuracy. A comparison of the grinding forces and roughness of the surfaces generated in dry and minimum quantity lubrication (MQL) conditions in both conventional grinding and optimal condition in UAG has been performed to identify the beneficial effects of providing vibration to the workpiece. The surface quality has been evaluated using 3D roughness data, 3D plots and SEM images of the ground surface. By examining nature of the ground surface and kurtosis ( $S_{ku}$ ) values of the surface profile, it has been concluded that UAG reduces brittle fracture and facilitates material removal by ductile mode for alumina. The desired condition of least machining forces and highest surface quality has been achieved during the combination of UAG and MQL.

**1. Introduction**

Advanced ceramics such as silicon nitride, silicon carbide, alumina etc finds application in high temperature applications, friction parts and as cutting tools [1, 2] due to their exceptional mechanical and thermal properties. Biomedical implants for dental and orthopedic applications are manufactured from alumina and zirconia ceramics and their composites. Even though ceramic components are manufactured by sintering process, the final shaping and finishing of ceramic components through grinding is inevitable [3]. Owing to their hard and brittle nature, grinding of advanced ceramic poses several challenges such as high cutting forces, edge chipping and formation of sub-surface cracks [4]. A hybrid method known as ultrasonic vibration assisted machining (UVAM or UAM) has gained attention for enhancing the machining quality of such materials [5]. UAM involves the addition of ultrasonic vibration to the tool or workpiece during conventional machining operation. Introduction of ultrasonic assistance to conventional machining processes change the monotonic nature of tool-workpiece interaction. This essentially alters the geometry, the nature of formation and separation of chips leading to reduction of machining forces and improvement of surface quality. The characteristic features that differentiate UAM from conventional machining methods have been summarised in [6, 7]. The application of ultrasonic vibration to conventional methods of drilling, milling and grinding has the potential to satisfy demands in various sectors (automotive, defense, nuclear, etc) while processing high-performance materials. Researchers have investigated a variant of UAM, ultrasonic vibration assisted grinding (UAG or UVAG) [8] to improve the grinding characteristics of hard-to-machine materials. Dambatta *et al* carried out an extensive review on the application of UAG to the processing of ceramics and aerospace alloys [9]. Based on several case

studies, they concluded that UAG technique is effective in minimizing machining forces, improving surface quality and enhancing tool life while grinding hard and brittle materials such as ceramics.

UAG involves the integration of an ultrasonic system that provides vibrations of small amplitudes (2–50  $\mu\text{m}$ ) to conventional grinding (CG). The application of UAG to process hard and difficult-to-grind materials has been shown to enhance surface quality, decrease the grinding forces and significantly reduce tool wear. Vibrations imposed on the workpiece or tool while grinding changes the dynamics of the process. Compared to the conventional grinding process, the path traced by the abrasive grits relative to the workpiece surface is altered, which has a direct impact on the forces generated and the ground surface quality. A kinematic model for understanding the contact paths of abrasive grains in UAG has been developed by Kitzig-Frank *et al* [10]. They concluded that, due to superimposed ultrasonic vibrations, the impact action of the abrasives on the workpiece surface results in higher material removal and reduction of cutting forces. Yang *et al* [11] proposed a contact rate model to study the nature of abrasive-workpiece interaction in UAG. Their analytical model shows that the periodic nature of separation between the abrasive and workpiece due to imposed vibration lowers the forces in UAG. Orthogonal grinding experiments considering four factors and four levels were carried out on  $\text{ZrO}_2$  ceramics to model surface roughness using a neural network model based on genetic algorithm. The reduction of surface roughness in UAG has been attributed to the reciprocating motion of abrasives and interference of adjacent grain trajectories. Zhou *et al* [12] proposed a novel parameter that can characterise the interference of grain trajectories during successive cycles of wheel rotation. The proposed parameter took into account the phase difference between ultrasonic vibrations due to wheel rotation. Due to this phase difference, the grooves formed by abrasive grits during the current cycle of wheel rotation interfere with the ones formed in the previous cycle. This results in higher material removal and leads to better surface topography in UAG. Application of UAG has shown to enhance the wear resistance of natural teeth and zirconia dental crowns by improving the lubrication retention (saliva) and contact properties of the ground surface [13].

Various theoretical models have been developed to model the cutting force, surface roughness and understand the mechanism of material removal in UAG [14–16]. These studies provide several insights into the kinematics of UAG responsible for its unique machining characteristics. When compared with the straight line motion of an abrasive grit in conventional grinding, the path traced by an abrasive grit in UAG is elliptical. This happens because of the provision of an additional motion to the tool/workpiece, which changes the path of abrasives relative to the workpiece surface. The number of abrasive grits coming into contact with the workpiece surface at a given point in time and engaging in the material removal process is also higher compared with the conventional grinding process. The high frequency vibration results in intermittent impact of the abrasive grains on to the workpiece surface. This causes splintering of abrasive grains, which results in a self-sharpening effect that maintains the grinding wheel sharp throughout the grinding process. The flattening of abrasive grains in CG increases the abrasive grit rubbing and plowing action on the workpiece, resulting in undesirable thermal effects that deteriorate the surface quality. It also renders the cutting process less efficient and increases the grinding forces. However in UAG, the superimposed vibrations keeps the wheel sharp leading to effective shearing of material, lowering tangential cutting force ( $F_t$ ). The sharp edges enable easier penetration of the abrasive grains on to the workpiece thereby reducing the normal force ( $F_n$ ) in grinding.

Chen Li *et al* [16] investigated the material removal mechanism of SiC ceramics during UAG using varied-depth nano-scratch tests. Based on the tests, they presented a detailed modelling of grinding forces in UAG. Correlation of data from orthogonal grinding experiments has been done by employing genetic algorithm. SEM images revealed that the primary mode of material removal in CG is chunk removal by brittle fracture, whereas UAG has favoured material removal by ductile mode. This has significantly improved the surface quality and reduced the depth of sub-surface cracks in samples processed by UAG. Zheng *et al* [17] have used 3D surface roughness and fractal geometry parameters to characterise SiCp/Al composites ground by ultrasonic vibration assisted end grinding. Grinding experiments as per  $L_{25}$  orthogonal array were performed using a metal bonded diamond grinding tool to study the effect of influencing factors on surface roughness. The surface roughness parameters they employed were found to improve with an increase in vibration amplitude. They arrived at an optimum condition which resulted in a minimum value of the area parameter roughness, Sq (root mean square roughness).

There have been attempts to enhance the characteristics of UAG process by using MQL technique. Application of MQL results in the formation of a surface film that reduces the friction and enables slipping of the abrasive grain. The atomised jet removes the heat generated at the grinding zone and enables effective removal of loose particles from the grinding zone. The separation machining characteristics of UAG has the capability to reduce the grinding force and enable better dissipation of heat from the region of contact. Hence a combination of both techniques is expected to result in better grinding characteristics. An experimental study of UAG in presence of MQL has been performed by Molaie *et al* [18]. They conducted grinding study on hardened AISI 52100 steel, with an objective to combine the beneficial effects of MQL with UAG. Their study shows that the periodic vibration in UAG allowed better penetration of the nanofluid lubricant to the grinding zone,

substantially reducing the grinding forces and surface roughness. An experimental study involving a combination of UAG with MQL on hardened bearing steel using nanoparticles has been conducted by Rabiei *et al* [19]. In addition to the lowering of grinding forces, UAG has eliminated surface burns by lowering the grinding temperature. The intermittent contact of abrasive grains during grinding has allowed efficient dissipation of heat which has reduced the undesirable thermal effects during grinding. Gao *et al* [20] has performed a study on the effect of combining 2D-UVAG with nanofluid-MQL on the MRR and surface characteristics on a nickel based alloy. The efficiency of nanofluid in performing its cooling and lubrication functions has been found to improve in UVAG due to the imposed vibrations. Also, 2D-UVAG has led to the generation of a surface with compact, uniformly distributed bulges and widened furrows leading to an even topography.

Hence it is established that UAG has the potential to overcome the difficulties while grinding ceramics by minimising the grinding forces and improving the surface quality. For ceramics, UAG reduces the amount of brittle fracture and promotes material removal through ductile mode. Researchers try to improve the UAG method by re-designing sonotrode, modifying the vibration characteristics, matching the ultrasonic system with the grinding parameters and altering the grinding environment. Even though there are several studies available in literature regarding the grinding of ceramics, they mostly rely on analytical models which require experimentally determined parameters. Literature suggests that, selection of a suitable combination of parameters is critical in achieving the desired effect of vibration assisted machining. Hence, a study aimed at the selection of optimum combination of UAG parameters satisfying multiple objectives needs to be done. The suitability and role of optimisation techniques to this stochastic process needs to be established.

Taguchi techniques are widely used in various areas for efficient planning of experiments and analysis of experimental data [21–24]. There are several statistical tools associated with it, which can be utilised to determine the influence of control factors and identify the optimum conditions. Signal to noise ratios (S/N ratios) calculated based on carefully designed experiments separates the effects of input parameters on response variables from those of noise factors. S/N ratio can be utilised to identify significance of factors and their effects on the responses. The analysis of variance (ANOVA) table, which shows the statistical influence of the factors on the output, can be used to identify the contribution of each factor towards the responses. M Emami *et al* [25] has utilised Taguchi mixed array based experimentation to select an optimum combination of the lubricant type and parameters, for grinding of alumina ceramic. The most influencing factors and their contributions were determined using the ANOVA table and selection of the optimal condition was achieved through S/N ratio analysis. Grey Relational Analysis (GRA) proposed by Deng [26] is one of the most commonly used approaches for analyzing real-world situations where a precise forecast is typically difficult. Taguchi based GRA is found to be effective for multi-objective optimisation of engineering problems and has been applied to optimise several processes. M Sarıkaya, and A Gullu conducted multiple response optimisation using Taguchi based GRA for turning operation of Haynes alloy in MQL condition [27]. Lohithaksha *et al* [28] have applied this method effectively for optimising end milling of Inconel 718 alloy. Taguchi-GRA optimisation employed by them has resulted in significant improvement of the process characteristics thereby confirming its effectiveness for multi-response problems. A similar methodology has been adopted by Rajyalakshmi and Venkata Ramaiah [29] for optimisation of wire EDM process. The optimised parameters selected by them has been found to enhance the machining performance. Selvakumar *et al* [30] have found the Taguchi-GRA optimisation method to be effective for improving the characteristics of turning process of aluminium metal matrix composite. Hence, Taguchi based GRA is an effective method for identifying the optimal parameters for multi-response problems and has been adopted in this work.

Even though research has been conducted on several aspects of UAG, further studies are required to corroborate the beneficial effects of UAG to enable its widespread application for ceramic materials. The effectiveness of improving UAG using MQL has to be investigated so as to obtain better surface quality while grinding of ceramics. Researchers mostly rely on average surface roughness parameter ( $R_a$ ) to evaluate the surface roughness in UAG. However, the need for assessment of surface quality using other parameters in conjunction with  $R_a$  for better assessment of surface quality in UAG has been emphasised in [31]. Such data for UAG of ceramic components is rarely available in literature. The current study aims to optimise the process parameters during UAG of alumina ceramic with an objective to simultaneously attain minimum grinding forces and improved surface finish. For this purpose, grinding experiments performed using Taguchi's orthogonal array have been optimised for identifying the desired conditions using GRA. A comparative study of the CG and UAG grinding characteristics is then carried out by performing grinding experiments under dry and MQL conditions. A proper assessment of the surface quality has been conducted using various surface texture parameters, SEM images and 3D plots.

## 2. Methodology

### 2.1. Background for selection of parameters

Material removal of alumina ceramics in conventional grinding is generally through brittle mode. Ductile regime machining and material removal with lower proportion of brittle fractures require grinding to be performed either at extremely high speeds or at very low depth of cuts [32]. In general, grinding process may be compared to material removal by multiple moving indenters. Generally, the forces in grinding are resolved into tangential cutting force ( $F_t$ ) and the normal force ( $F_n$ ). Tangential force determines the power expended in grinding. The normal load denotes the ease of penetration of abrasive grits into the workpiece and its magnitude is dependent on the grit depth of cut. As the depth of cut increases the normal force increases. This is expected to increase the depth of sub-surface cracks formed during grinding of ceramics, leading to flexural strength reduction. A fundamental study on grinding damage mechanism in ceramics using static and moving indenters has been performed by Malkin *et al* [33]. They observed that grinding of ceramics above critical depth of cut leads to degradation of strength. This may be attributed to the formation of median cracks due to indentation of abrasive grits on the workpiece surface, which extends below the surface and retained in the sub-surface after grinding. The depth of the median cracks has been found to be dependent on the normal load, which in turn depends on the depth of indentation (equivalent to depth of cut in grinding). Hence depth of cut in grinding plays a very important role in determining the surface quality and residual strength properties of ceramic workpieces.

Ostasevicius *et al* [34] performed a comparative study on the impact of providing vibrations to the tool and workpiece on the surface quality of tungsten carbide ceramic while grinding. Based on SEM micrographs and  $R_a$  values of ground samples, they concluded that UAG with excitation of workpiece reduced the brittle fracture while grinding and yielded better surface quality. It has also removed the restrictions on tool rotation speed and vibration frequencies that could be employed for UAG. Even when vibrations were provided to the workpiece, grinding at low depth of cuts (less than 5  $\mu\text{m}$ ) has deteriorated the quality UAG due to unstable tool-workpiece contact and micro-impact action.

Low values of depth of cuts ensured better surface quality in CG when compared to UAG. However as depth of cut increased, the surface roughness has been found to increase in CG whereas the surface quality improved in UAG.

From these studies it may be concluded that the depth of cut used while grinding of hard and brittle ceramics should be chosen judiciously. To ensure good surface quality in UAG, the depth of cuts should be moderate depending on the ceramic being ground. Also configuring the UAG set up for providing vibrations to the workpiece is recommended. In addition to these aspects, the selection of process parameters for UAG of alumina has been done considering the inferences from research on grinding of ceramics mentioned in table 1. Based on the references cited in the table, it can be concluded that grinding parameters such as feed rate, depth of cut, and cutting speed greatly influence the grinding forces and surface roughness. UAG facilitates processing at higher feed rate and depth of cut ensuring better grinding characteristics under these conditions. The effect of varying the vibration amplitude and cutting speed also needs to be understood. So the factors considered for optimisation of UAG are cutting speed, feed rate, depth of cut and vibration amplitude.

### 2.2. UAG Set up and details of experiments done

The experimental study has been planned in two stages. Initial stage of experimentation is aimed at studying the effect of process parameters and identifying the optimum combination of parameters for the current UAG set-up. Taguchi's technique being an effective way of planning experiments which ensures efficient utilisation of resources, has been adopted for conducting the experiments. Experimentation using Taguchi L18 mixed array has been chosen for obtaining the data required for optimisation. Considering the inferences given in table 1 and the processing capability of the machine tool, the parameter levels for experimentation have been fixed as listed in table 2(a). Using the results from these experiments, optimum parameter combination has been identified. In the next stage of experimentation, UAG has been performed in dry and MQL conditions using the optimum set of parameters. Conventional grinding (CG) tests have also been performed for comparative study. The MQL parameters used for the experimentation are based on the recommendations by Emami *et al* [37] and are mentioned in table 2(b). Mathematical models were developed for the output parameters using regression analysis and have been used to predict responses at the optimal parameter combination.

The grinding experiments have been performed in ALEX NH 500 surface grinder using a diamond grinding wheel. After each experiment, wheel dressing has been performed with an abrasive dressing stick. The details of the grinding wheel and dressing stick are listed in table 2(b). Ceramic samples of sintered alumina measuring 70 mm  $\times$  20 mm  $\times$  10 mm were procured from HiTech Ceramics, Chennai. SEM image of alumina workpiece is given in figure 1. Its properties and composition as received from the supplier are given in table 3. In order to

**Table 1.** Reference works utilised for selection of machining parameters.

Paper title	Machining conditions		Inferences
Predicting subsurface damage in silicon nitride ceramics subjected to rotary ultrasonic assisted face grinding Baraheni, M and Amini, S (2019) [35]	Vibration Parameters Material Feed Speed Depth of Cut Grinding tool	20 kHz, 10 $\mu\text{m}$ amplitude  Si <sub>3</sub> N <sub>4</sub> ceramic 3, 6, 8, 12, 16, 24 ( $\text{mm min}^{-1}$ ) 1000–6000 rpm; Tool Outer Diameter 6 mm 30, 40, 60, 80, 100, 120 ( $\mu\text{m}$ ) Diamond grinding pin, Mesh size D125	Least sub-surface damage has been obtained for highest value of cutting speed and lowest values of feed rate and depth of cut
Investigating the Minimum Quantity Lubrication in grinding of Al <sub>2</sub> O <sub>3</sub> engineering ceramic Emami <i>et al</i> (2014) [25]	Feed Speed Depth of Cut MQL Liquid Flow rate MQL Air Flow rate Grinding tool	9, 12, 16, 21 $\text{m min}^{-1}$ 30 $\text{m s}^{-1}$ 8, 12, 18, 27 ( $\mu\text{m}$ ) 150 $\text{ml h}^{-1}$ 30 $\text{l min}^{-1}$ Metal Bonded Diamond wheel, Grain sizes D91 and D181	<ul style="list-style-type: none"> <li>Depth of cut is the most significant factor that influences the grinding forces and surface roughness.</li> <li>Employing high feed rate can lower specific energy and improve the productivity</li> <li>However higher feed rates can result in higher R<sub>a</sub> values</li> </ul> <p>Hence grinding at a combination of high feed rate and low depth of cut has been recommended</p>
Study on key factors influencing the surface generation in rotary ultrasonic grinding for hard and brittle materials Wang <i>et al</i> (2019) [36]	Vibration Parameters Material Feed Speed Depth of Cut Grinding tool	Frequency 20 kHz , Amplitudes 4,6,8,10 ( $\mu\text{m}$ ) Si <sub>3</sub> N <sub>4</sub> ceramic 100 $\text{mm min}^{-1}$ 2500–3000 rpm, Tool Outer Diameter 5 mm 10 $\mu\text{m}$ Diamond grinding pin, Mesh size 150 #	<ul style="list-style-type: none"> <li>Lower cutting velocity has resulted in better surface finish, as it ensures separation machining characteristics in UAG and overlapping of grain trajectory</li> <li>Higher cutting velocity requires higher vibration amplitude to satisfy this condition.</li> </ul>

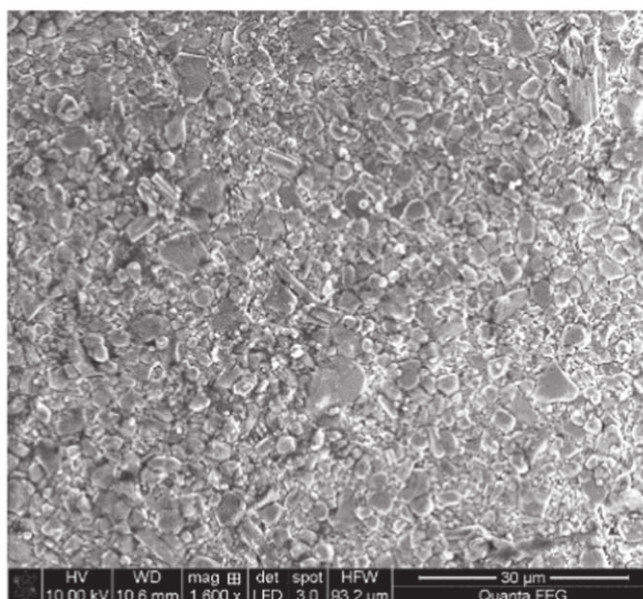


**Figure 1.** SEM image and of alumina sample as received.

**Table 2.** (a) Factors and levels for Taguchi's mixed array and (b) grinding wheel properties and MQL parameters.

Parameters for L18 Array		
Array	Levels	Unit
Amplitude, ( $A$ )	6, 12	microns
Feed, ( $V_w$ )	19, 20, 21	$\text{m min}^{-1}$
Wheel Speed, ( $V_s$ )	10, 20, 30	$\text{m s}^{-1}$
Depth of Cut, ( $a_e$ )	10, 16, 22	$\mu\text{m}$
Grinding Wheel	Diamond abrasive Metal Bonded wheel D200-U10-X3	
Mesh size	100/120	
MQL Parameters	Neat oil supplied at the rate of $150 \text{ ml hr}^{-1}$ , Air Pressure maintained at 4 bar	
Abrasive Dressing Stick	WIL 2 DRST ITO 038	

**Table 3.** Composition and Properties of alumina ceramic.

Grade	$\alpha$ - alumina	
Composition	$\text{Al}_2\text{O}_3$	99.50%
	$\text{SiO}_2$	0.10%
	$\text{Fe}_2\text{O}_3$ ,	0.10%
	$\text{CaO} + \text{MgO}$	0.15%
	$\text{K}_2\text{O} + \text{Na}_2\text{O}$	0.15%
Apparent Density	$\sim 3.89 \text{ g/cc}$	
Hardness (Vickers)	1800 HV	
Elastic Modulus	380 GPa	
Bending Strength	300 MPa	
Maximum Working Temperature	1800 °C	

provide ultrasonic vibrations to the workpiece, an ultrasonic generator has been integrated with the grinding machine as shown in figure 2. The ultrasonic generator gets input current at 230V/50 Hz & generates mechanical vibrations. A piezoelectric crystal present in the ultrasonic stack assembly converts the electrical

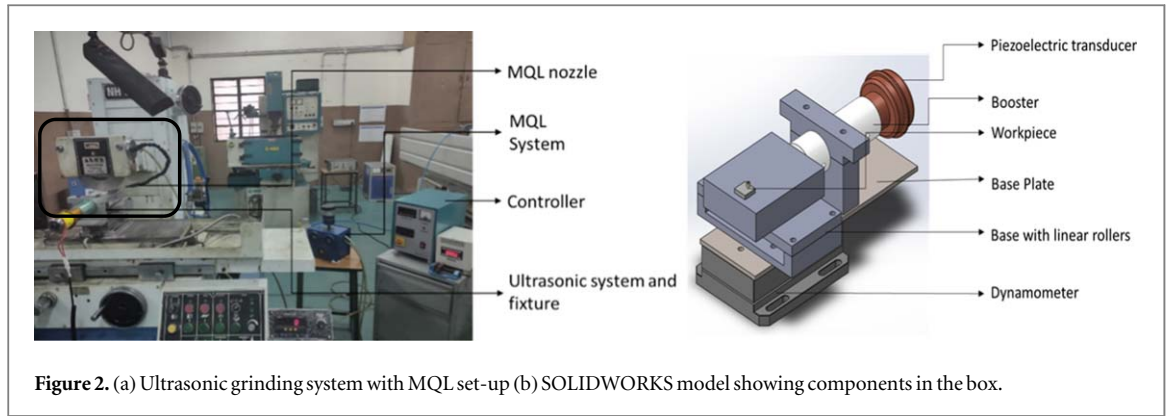


Figure 2. (a) Ultrasonic grinding system with MQL set-up (b) SOLIDWORKS model showing components in the box.

signal input into mechanical vibrations at a frequency of 20 kHz, which is then transferred to the sonotrode via a booster. A controller is used to set the desired vibration amplitude, while the frequency of vibration remains constant. The controller has a rotary switch to increase the vibration amplitude from 6 to 12  $\mu\text{m}$  in steps of 2  $\mu\text{m}$ . The workpiece is mounted on a rectangular block sonotrode placed on top of a frictionless base. The base consists of linear flat rollers which allows the set up to vibrate with minimal losses (figure 2(b)). The whole vibrating set up is mounted on top of the dynamometer via a base plate. For conventional grinding tests, the ultrasonic system is turned off.

Researchers have used different configurations for converting a conventional grinding machine into UAG system. UAG set up may be designed for vibrating either tool or the workpiece. However it is preferable to vibrate the workpiece because it allows for easier incorporation of vibrating system into the conventional machine tool and provides greater stability with regards to the rotating spindle [15]. In the current work, the vibrations are provided to the workpiece fixture. The UAG system is configured in such a way that the workpiece vibrates in the direction perpendicular to the in-feed. No cross feed movement has been provided to the work table. The normal and tangential forces during grinding have been recorded using a multi-component dynamometer, Kistler 9257B. The surface roughness values have been measured using MarSurf GD 120 roughness measuring system. The surface characteristics have been assessed using SEM images of the ground surface. The surface topography has been examined using 3D plots generated by Taylor Hobson's non-contact 3D surface profiler, Talysurf CCI 3000, working on the principle of advanced optical interferometry.

### 2.3. Determination of optimum parameters

The optimum machining conditions are obtained by the grey relational analysis (GRA). GRA converts complicated multiple response problem to optimisation of a single attribute called the grey relation grade (GRG). The procedure for performing GRA given by M Sarikaya *et al* [27] and Rajyalakshmi *et al* [29] has been adopted. The steps followed are as given below:

**Step 1.** Normalisation of the responses is done to bring the data in the range 0–1. This is also known as generation of comparability sequence. The responses selected are  $F_t$ ,  $F_n$  and  $R_a$ . A lower value is desired for these responses, hence the normalisation is done based on the smaller-the-better criterion using equation (1).

$$y_{n,j}(p, j) = \frac{\max(y_{p,j}) - y_{p,j}}{\max(y_{p,j}) - \min(y_{p,j})} \quad (1)$$

where,  $y_n(p, j)$  denotes the normalised value of the  $p^{\text{th}}$  response characteristic for the  $j^{\text{th}}$  experiment  $y_{p,j}$ ,  $\max(y_{p,j})$  and  $\min(y_{p,j})$  represents the maximum and minimum  $y_j$  values for the  $p^{\text{th}}$  response.

**Step 2.** The next step is determination of deviation sequences. This is calculated using equation (2).

$$\Delta_0(p, j) = |y_{0n}(p) - y_n(p, j)| \quad (2)$$

where  $\Delta_0(p, j)$  is the absolute difference of the normalised values of reference sequence  $y_{0n}(p)$  from the comparability sequence  $y_n(p, j)$ .

**Step 3.** This is followed by estimation of grey relational coefficient (GRC). GRC ( $\xi$ ) can be obtained using equation (3):

**Table 4.** Results from Taguchi L 18 experimentation for alumina.

Expt no	Amplitude A ( $\mu\text{m}$ )	Feed $V_w$ ( $\text{m min}^{-1}$ )	Wheel speed $V_s$ ( $\text{m s}^{-1}$ )	Depth of cut $a_e$ ( $\mu\text{m}$ )	Tangential force, $F_t$ (N)	Normal force, $F_n$ (N)	Surface roughness $R_a$ ( $\mu\text{m}$ )
1	6	19	10	10	56	154	1.754
2	6	19	20	16	64	206	1.707
3	6	19	30	22	68	197	1.750
4	6	20	10	10	66	198	1.728
5	6	20	20	16	79	292	1.778
6	6	20	30	22	73	210	1.751
7	6	21	10	16	86	267	1.818
8	6	21	20	22	77	217	1.820
9	6	21	30	10	64	203	1.742
10	12	19	10	22	62	196	1.772
11*	12	19	20	10	52	147	1.621
12	12	19	30	16	52	150	1.648
13	12	20	10	16	65	188	1.738
14	12	20	20	22	62	230	1.801
15	12	20	30	10	56	182	1.565
16	12	21	10	22	76	234	1.796
17	12	21	20	10	62	171	1.684
18	12	21	30	16	55	165	1.702

$$\xi_j(p) = \frac{\Delta_{\min} + \zeta \Delta_{\max}}{\Delta_0(p, j) + \zeta \Delta_{\max}} \quad (3)$$

here,  $\Delta_{\max}$  and  $\Delta_{\min}$  are the maximum and minimum values of  $\Delta_0$ .  $\zeta$  is known as distinguishing coefficient, whose value is generally taken as 0.5.

**Step 4.** Finally the grey relational grade (GRG) is determined. The analysis of the multi-objective problem is thus converted to analysis of the characteristic, GRG. GRG ( $\gamma_j$ ) is computed as the average of GRC of individual responses as:

$$\gamma_j = \frac{1}{n} \sum_{p=1}^n W_j \xi_j(p) \quad (4)$$

here,  $W_j$  is the weighting factor for GRC.

While calculating the GRG, equal weightage has been considered for all the attributes. Since the number of attributes considered here is 3, the weighting factor  $W_j = 1/3$ . Higher the GRG, closer the experiment is to the optimum conditions. The average GRG at the individual level of each factor may also be computed. The optimal levels are then determined on the basis of average GRG computed for individual factor levels.

### 3. Optimisation results and regression modelling

#### 3.1. Selection of optimum condition

The results obtained from grinding experiments have been tabulated in table 4. Figure 3 shows the alumina workpieces before and after performing grinding operation. The normal force ( $F_n$ ), tangential force ( $F_t$ ) and average surface roughness ( $R_a$ ) are given for each experimental run. These responses are then utilised for optimisation of parameters using GRA. The computation of normalised responses, GRC and GRG for responses from UAG of alumina are given in table 5. The experiments conducted have been ranked in the order in which they are closer to the optimum conditions. It can be seen from table 5 that experiment 11 has the GRG value closer to 1 and is thus nearer to the optimum condition. The parameters and levels corresponding to this experiment can be seen from table 4. For experiments, the rank was assigned in the decreasing value of GRG. The effect of each UAG parameter on the output variables and the selection of optimum combination of parameters are done using response plots of average GRG at each level. For this, the multi-response problem is analysed using a single response characteristic, which is the average GRG. The GRG value for each experiment is taken as the response and the analysis is performed using MINITAB 17. The main effects plot of mean GRG at each level for the factors is shown in figure 4. The optimum level for each factor is the one corresponding to highest GRG. Based on the main effects plot in figure 4, the optimum levels for the parameters are: amplitude–Level 2, feed–

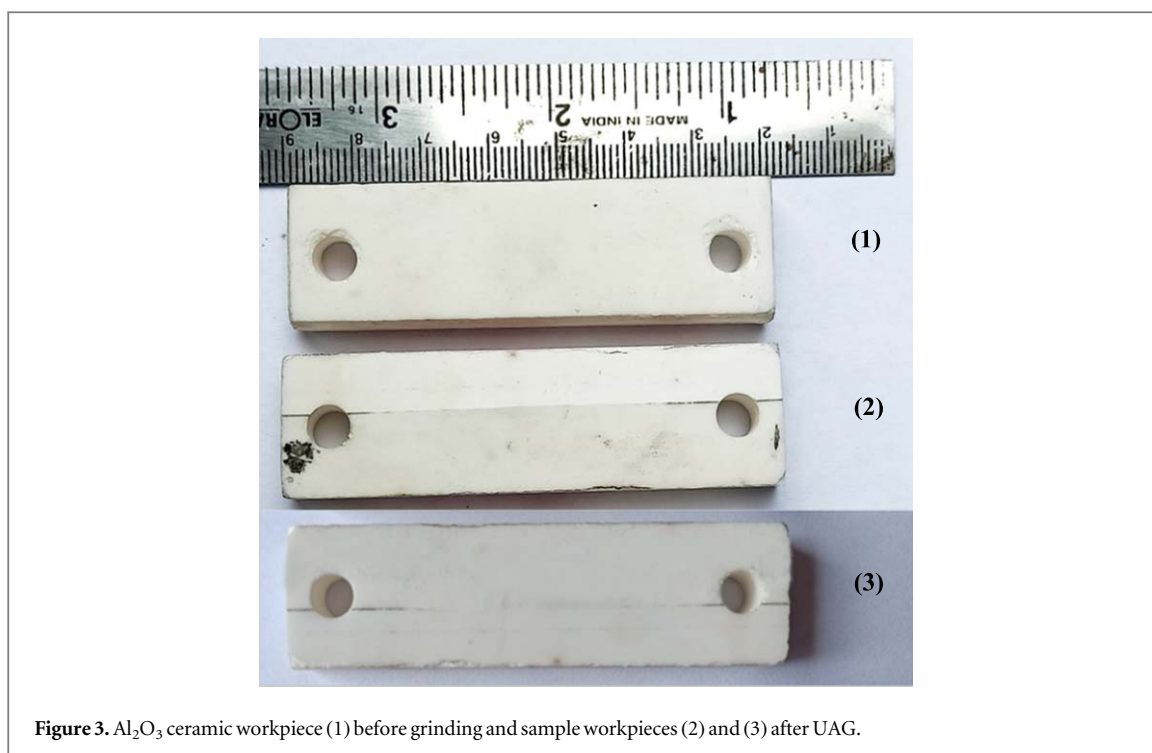


Figure 3. Al<sub>2</sub>O<sub>3</sub> ceramic workpiece (1) before grinding and sample workpieces (2) and (3) after UAG.

Table 5. Calculation of Grey relational grade of UAG responses for Alumina.

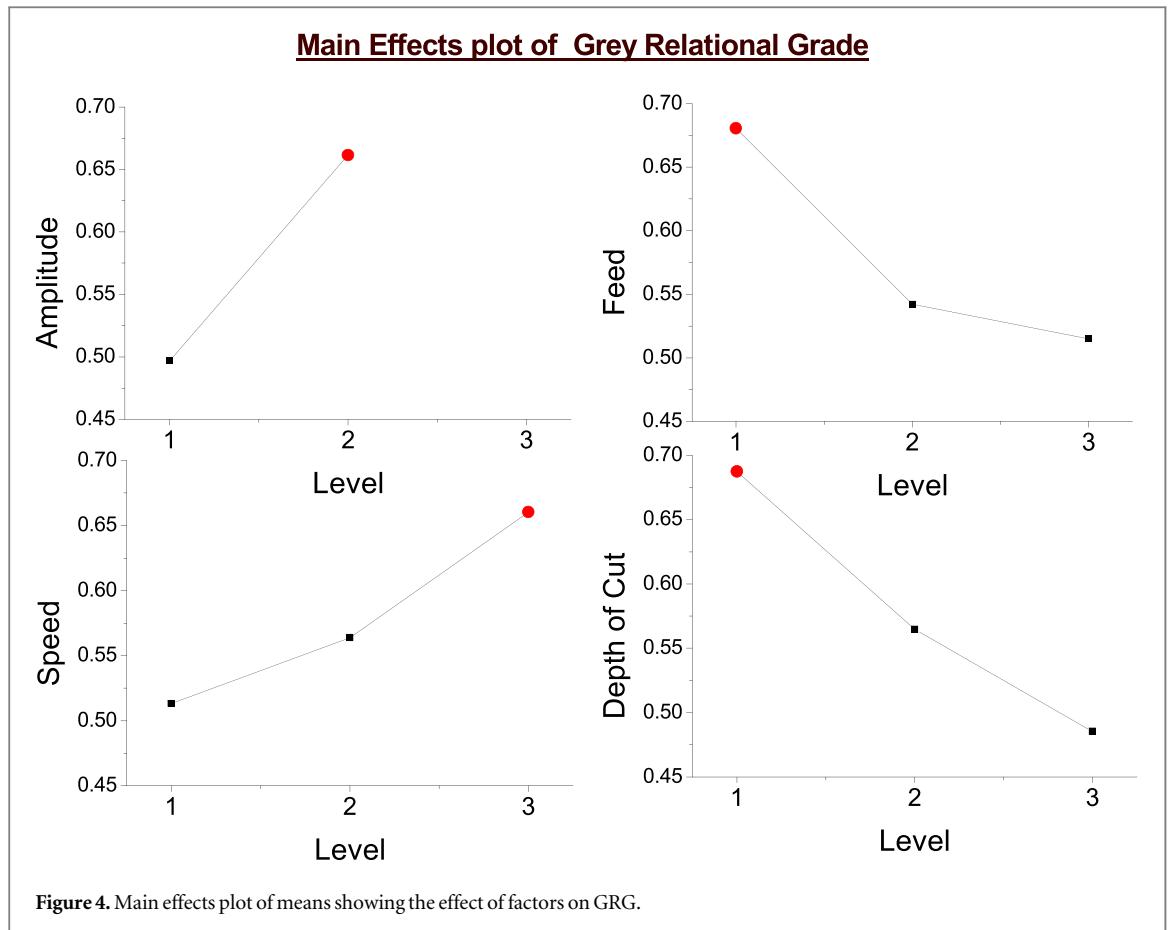
Expt. no	Normalised responses			Grey relational coefficients ( $\xi$ )			GRG ( $\gamma_j$ )	Rank
	$F_t$	$F_n$	$R_a$	$F_t$	$F_n$	$R_a$		
1	0.877	0.946	0.215	0.803	0.902	0.389	0.698	5
2	0.661	0.590	0.499	0.596	0.550	0.500	0.548	8
3	0.529	0.654	0.448	0.515	0.591	0.475	0.527	11
4	0.587	0.648	0.339	0.548	0.587	0.431	0.522	12
5	0.211	0.000	0.151	0.388	0.333	0.371	0.364	17
6	0.382	0.561	0.542	0.447	0.532	0.522	0.500	13
7	0.000	0.174	0.000	0.333	0.377	0.333	0.348	18
8	0.264	0.514	0.217	0.405	0.507	0.390	0.434	15
9	0.646	0.609	0.370	0.585	0.561	0.443	0.530	10
10	0.712	0.658	0.263	0.634	0.594	0.404	0.544	9
11*	1.000	1.000	0.801	1.000	1.000	0.715	0.905	1
12	0.998	0.977	0.705	0.997	0.956	0.629	0.861	2
13	0.617	0.714	0.385	0.566	0.636	0.448	0.550	7
14	0.705	0.428	0.160	0.629	0.466	0.373	0.489	14
15	0.881	0.758	1.000	0.808	0.674	1.000	0.827	3
16	0.307	0.397	0.182	0.419	0.453	0.379	0.417	16
17	0.705	0.834	0.587	0.629	0.751	0.548	0.643	6
18	0.910	0.874	0.510	0.848	0.799	0.505	0.717	4

Level 1, wheel speed–Level 3 and wheel depth of cut–Level 1. From table 2(a), this corresponds to the parameter combination of  $A$ : $-12 \mu\text{m}$ ,  $V_w$ : $-19 \text{ m min}^{-1}$ ,  $V_s$ : $-30 \text{ m s}^{-1}$  and  $a_c$ : $-10 \mu\text{m}$ .

This indicates that the optimum UAG conditions are achieved at lower feed rate, smaller depth of cut, higher cutting speed and at higher value of ultrasonic vibration amplitude. The result is in accordance with that reported by M Baraheni *et al* [38].

Contrary to the data obtained in [36] given in table 1, the optimum condition has occurred when the cutting speed is maximum. This result can be justified as follows:

UAG processing using an experimental set-up in which the vibrations are applied tangential to the wheel speed (tangential UVAG) needs to satisfy a critical condition depending on the processing parameters. This is essential to ensure periodic separation of abrasive-workpiece contact in grinding that differentiates UAG from CG. The vibration amplitude and frequency required to ensure the separation machining characteristic in tangential UVAG



depends on the wheel velocity and feed rate employed for grinding [11]. In such systems, employment of higher cutting speeds requires ultrasonic vibrations to be provided at higher frequency and amplitude to ensure separation grinding process. However satisfying the critical condition in a UAG system is not required when vibrations are provided to the workpiece, perpendicular to the direction of cutting velocity [39]. When the experimental set-up is configured in this manner, grinding may be performed at higher cutting velocities, as satisfying the critical condition is not essential for achieving the interrupted cutting characteristic of UAG. The UAG system used for experiments in this study is configured in such a way that vibrations are provided to the workpiece in the horizontal plane, perpendicular to the direction of cutting velocity. Hence higher cutting speeds could be used in the experiments without being constrained by the critical condition for UAG at the frequency and amplitude used. This has resulted in lower forces and better  $R_a$  values at a higher wheel speed of  $30 \text{ m s}^{-1}$ .

In order to understand the degree of influence of factors on the responses, the S/N ratio analysis has been performed for average GRG. As a higher value is desirable for GRG, the main effects of S/N ratios have been plotted using MINITAB 17 for larger – the – better characteristic in figure 5. The main effects plots are oriented vertically with respect to the mean line, which denotes that the effect of factors are significant. Steeper slope of a line in main effects plot for S/N ratios signify the higher impact of the corresponding factor on the response. In this case, every factor can be seen to have a significant effect on GRG. The data points corresponding to highest values of S/N ratios for GRG of each parameter denote the optimum level. The steepness of the S/N ratio plots show the impact of varying the input variables on the response parameters.

### 3.2. Development of regression models

Mathematical modelling is done using regression analysis in MINITAB 17 for normal force ( $F_n$ ), tangential force ( $F_t$ ) and surface roughness ( $R_a$ ). The mathematical models developed are given below :

*Tangential force ( $F_t$ ):*

$$F_t = -1540 + 1.44A + 142.0V_w + 7.86V_s + 8.14a_e - 3.17V_w^2 - 0.0022V_s^2 - 0.0471a_e^2 \\ - 0.056A * V_w - 0.0178A * V_s - 0.1269A * a_e - 0.361V_w * V_s - 0.186V_w * a_e \\ - 0.0556V_s * a_e$$

$$R^2 = 96.35\%$$

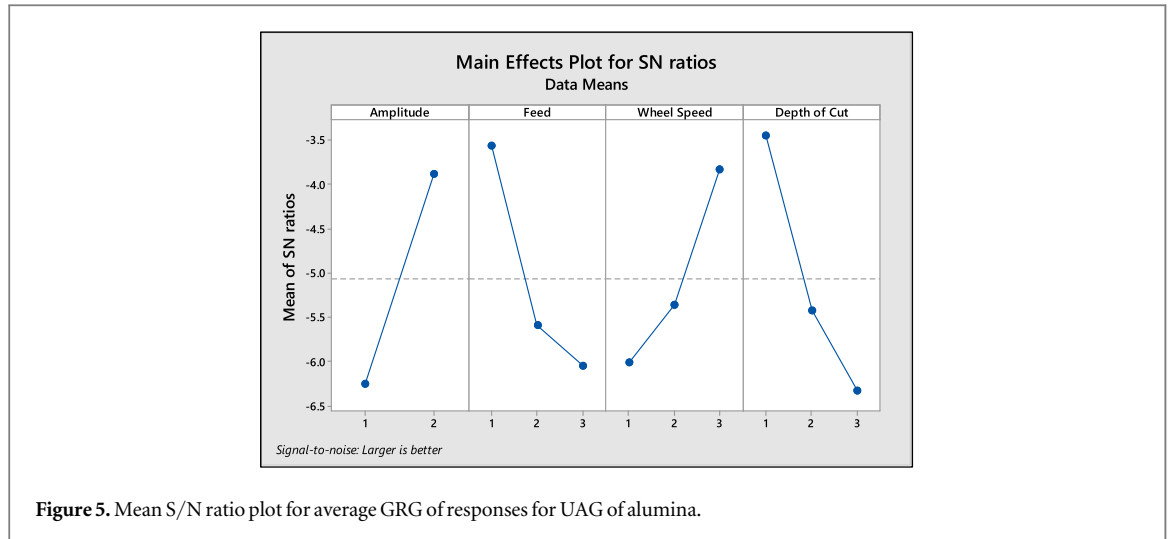


Figure 5. Mean S/N ratio plot for average GRG of responses for UAG of alumina.

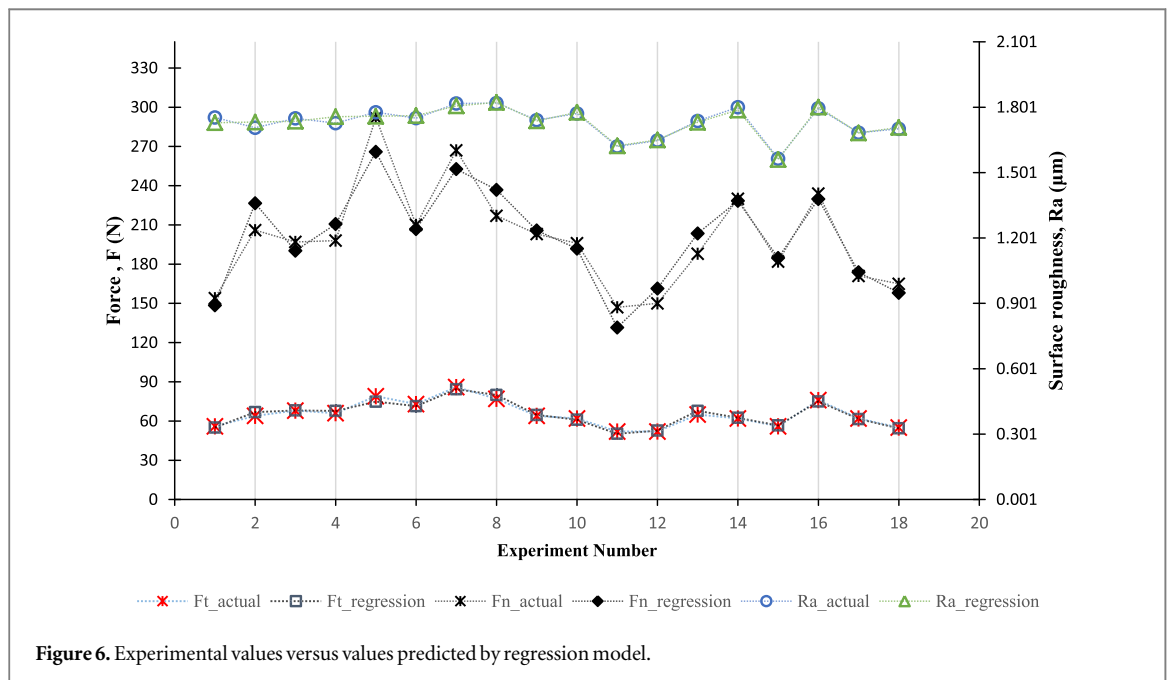


Figure 6. Experimental values versus values predicted by regression model.

Normal force ( $F_n$ ):

$$F_n = -13498 - 30.6A + 1300V_w + 41.7V_s + 46.8a_e - 31.1V_w^2 - 0.196V_s^2 - 0.296a_e^2 + 0.77A * V_w + 0.141A * V_s + 0.262A * a_e - 1.45 V_w * V_s - 1.39V_w * a_e - 0.448V_s * a_e$$

$$R^2 = 89.51\%$$

Average Surface Roughness ( $R_a$ ):

$$R_a = 6.23 + 0.0321A - 0.496V_w - 0.0096V_s + 0.0111a_e + 0.0140V_w^2 - 0.000199V_s^2 - 0.000141a_e^2 - 0.00289A * V_w - 0.000260A * V_s + 0.001502A * a_e + 0.00053V_w * V_s - 0.00103V_w * a_e + 0.000422V_s * a_e$$

$$R^2 = 95.91\%$$

$R^2$  values of the regression models are high, suggesting a good fit of the mathematical models with the experimental data. The experimental values versus estimated values for the output variables are plotted in figure 6. It can be seen that both values agree well showing the effectiveness of prediction. The regression models can thus be used for precise response predictions for any given combination of factors.

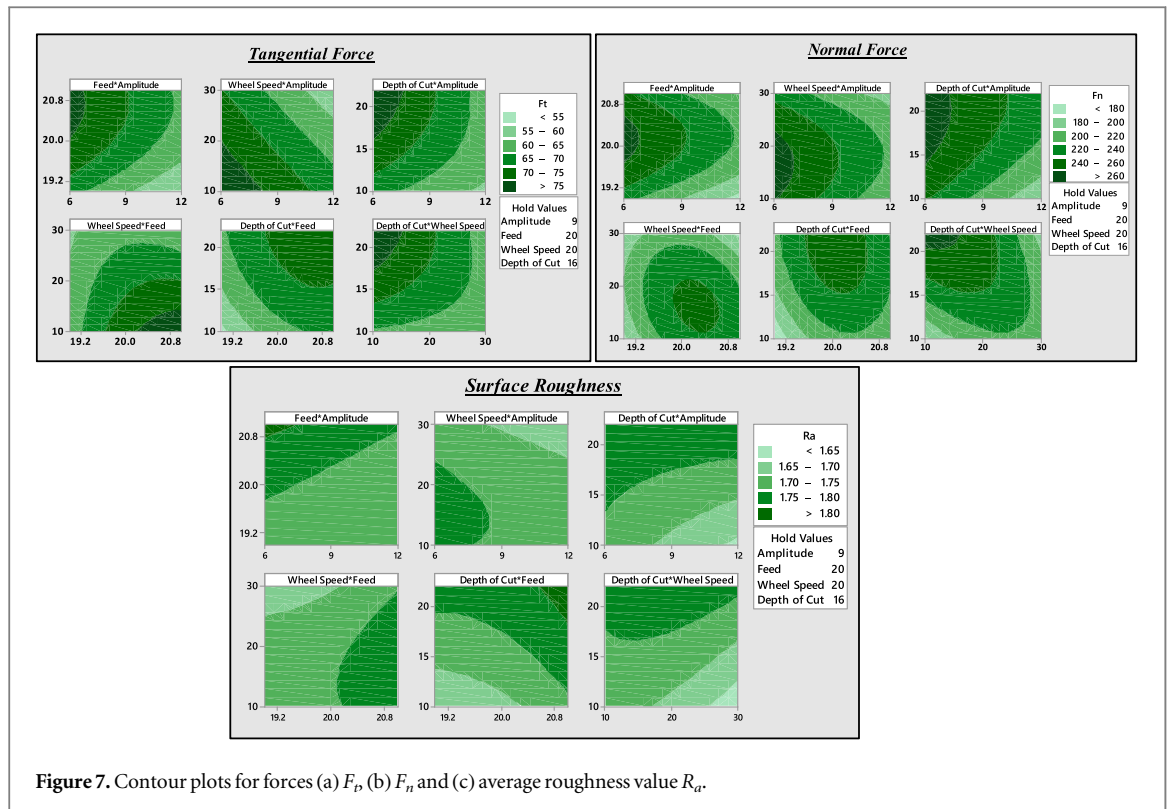


Figure 7. Contour plots for forces (a)  $F_t$ , (b)  $F_n$  and (c) average roughness value  $R_a$ .

Contour plots generated using the regression models are given in figure 7. The plot can be used to analyse the influence of input parameters on  $F_t$ ,  $F_n$  and  $R_a$ . The optimal conditions of lower forces and surface roughness values are towards the lighter shade of the contour plot. Irrespective of the grinding parameter used, the values of forces and surface roughness are lower when the vibration amplitude is  $12 \mu\text{m}$ , the highest level. As expected, the  $F_t$ ,  $F_n$  and  $R_a$  values are minimum at a lower feed rate and depth of cut. Some researchers have observed that the effect of ultrasonic amplitude in UAG diminishes at higher values of feed and depth of cut [2]. However selection of vibration amplitude matching the grinding parameters needs to be done to obtain the positive effect of UAG [25]. This is required especially while grinding at higher values of feed rate and depth of cut, as such conditions can conceal the effect of vibrations applied. However from the contour plots it can be inferred that provision of adequate vibrations to the workpiece has a beneficial effect even when grinding at higher values of feed rate and wheel depth of cut. The contour plots indicate the role of parametric optimisation in identifying the suitable combination of parameters in UAG. The benefits of UAG can be ensured by selecting a vibration amplitude suitable to the conventional grinding parameters.

Addition of vibrations to conventional grinding has a significant effect on surface roughness. According to the contour plots, it can be seen that application of vibration amplitude above  $9 \mu\text{m}$  ensures lower values of  $R_a$ . Grinding at depth of cuts above  $15 \mu\text{m}$  can result in higher values of grinding forces and surface roughness. Wheel speed above  $20 \text{ m s}^{-1}$  facilitates the reduction of force and roughness values. Particularly, a wheel speed of  $30 \text{ m s}^{-1}$  ensures lower forces and better  $R_a$ , even at higher feed rates and depth of cuts. A combination of higher wheel speed and higher amplitude is recommended for achieving better surface quality as it may be seen from the contour plot for surface roughness. It is commonly understood that for higher material removal in grinding, higher feed rate and depth of cut is necessary. At the same instance, higher grinding depth and feed rate result in higher cutting forces and roughness values. However the analysis done shows that optimisation of UAG will result in a suitable combination of parameters ensuring better grinding characteristics without compromising on productivity. Thus the contour plots show that better performance in UAG occurs at conditions of higher vibration amplitude, cutting speed, lower values of feedrate and depth of cut.

### 3.3. Analysis of variance (ANOVA)

The significance of the parameters on the average GRG values can be found using ANOVA table. The ANOVA analysis for average GRG of the responses is listed in table 6. The statistical significance of the responses can be identified from the  $F$  statistic and  $p$  value given in the ANOVA table. A larger  $F$  value indicates higher significance of the corresponding machining parameter towards the responses. The percentage contribution of each factor towards the GRG for the multiple responses is given in the last column.

**Table 6.** ANOVA table of GRG for grinding test of alumina.

Source	Degrees of freedom	Sum of squares	Mean sum of squares	F ratio	p value	Percentage contribution
Amplitude	1	0.12202	0.12202	25.07	0.001	27
Feed	2	0.09473	0.04737	9.73	0.005	21
Wheel Speed	2	0.06707	0.03354	6.89	0.013	15
Depth of Cut	2	0.12469	0.06235	12.81	0.002	27
Residual Error	10	0.04866	0.00487			
Total	17	0.45718				

**Table 7.** Predicted values and experimental values at the optimum levels.

Response variable	Predicted value	Observed value	Deviation (%)
Tangential Force, $F_t$	52	49	5.77
Normal Force, $F_n$	146	134	8.22
Roughness, $R_a$	1.540	1.435	6.82

It can be seen that the contribution of vibration amplitude is 27%. This shows that the influence of ultrasonic vibration amplitude on the responses is significant. The influence of depth of cut and feed rate is 27% and 21 % respectively. This is followed by wheel speed with its contribution at 15%. The effects of all parameters on the GRG for the combined responses are statistically significant, as all the  $p$  values are below 0.05.

### 3.4. Confirmation experiments

Once the optimum levels of parameters have been identified, a confirmation experiment has been performed. The values of  $F_t$ ,  $F_n$  and  $R_a$  predicted by regression equations and those observed from experiments at the optimum level of parameters shall be compared from table 7. The two sets of values are reasonably close, suggesting that regression modelling of forces and roughness based on experimental values is effective. This shows that Taguchi based GRA is suitable for identifying the optimum parameter combination for UAG.

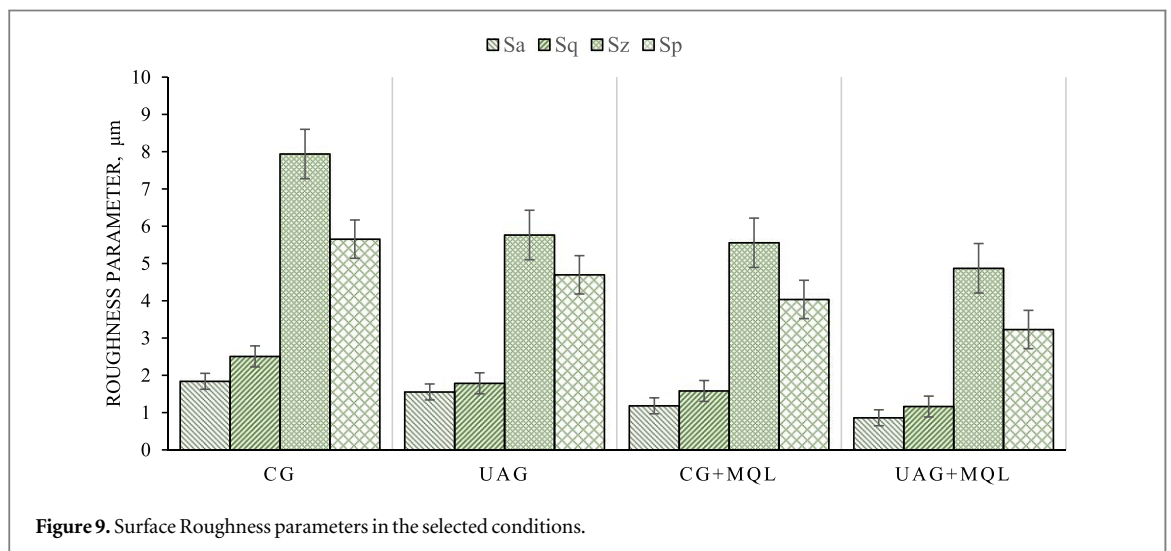
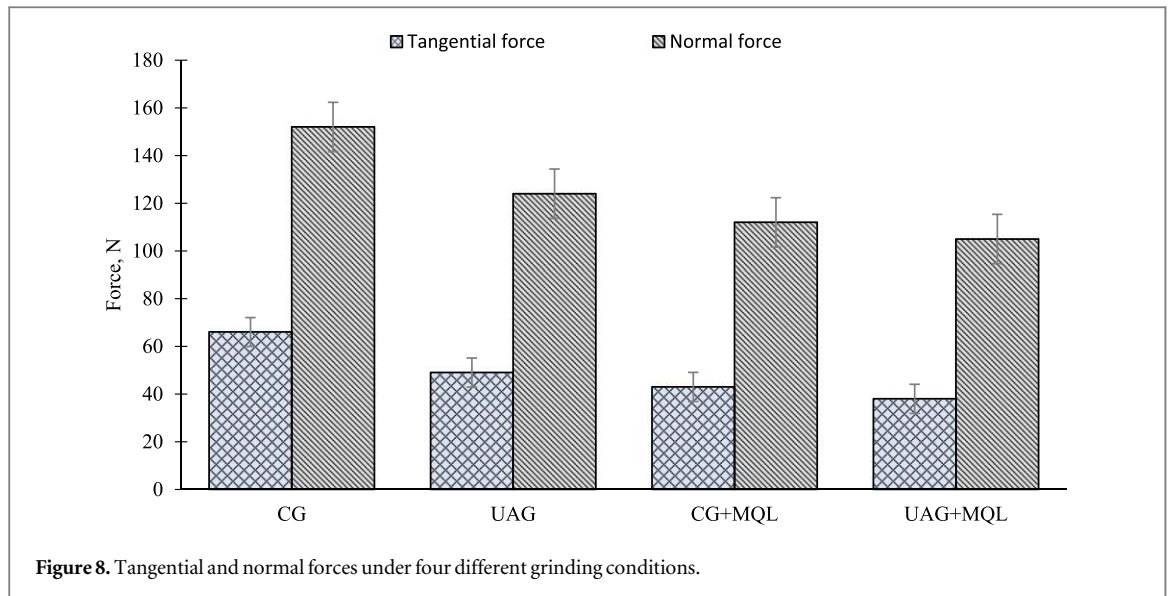
## 4. Comparison of UAG with CG at different grinding conditions

A new set of experiments is performed once the optimum conditions are identified. To analyse the combined action of UAG and MQL, grinding tests have been performed at the optimum parameters in MQL condition. For this, a jet of atomised cutting fluid obtained by mixing oil at  $150 \text{ ml h}^{-1}$  and pressurised air at 4 bars using an MQL set-up, is directed towards the grinding zone through a nozzle as shown in figure 2(a). Conventional grinding (CG) experiments have also been performed in the dry and MQL conditions for comparison with the corresponding UAG tests.

### 4.1. Analysis of grinding forces

The grinding forces are compared for different grinding conditions in figure 8. The values of tangential and normal forces are highest for CG performed in dry environment. It can be observed that there is a significant reduction of grinding forces in UAG. The presence of high frequency vibration results in continuous impact of the abrasive grits on to the workpiece resulting in self-sharpening of grains during grinding. This keeps the grinding wheel sharp, enabling the abrasives to penetrate into the alumina workpiece easily, thereby lowering the normal force in UAG. In UAG, abrasive grain's trajectories overlap which reduces the chip size in grinding [36]. Provision of vibrations during grinding also results in variations in uncut chip thickness [18], which lowers the tangential grinding forces. These effects, which occur due to the ultrasonic vibrations superimposed on to the workpiece, are absent in CG. As a result, the grinding forces will be higher in CG compared to UAG.

Application of MQL results in the formation of a stable tribofilm at the grinding contact zone which lowers the friction during grinding. This effectively make the material removal process easier by lowering the tangential force required in MQL grinding condition [37]. The grinding force values are lowest during UAG in presence of MQL. UAG + MQL condition (figure 8) has resulted in reduction of tangential force by 42% and normal force by 31% when compared with CG, which is substantial. The periodic separation of abrasive-workpiece contact is a feature of UAG that reduces the friction while grinding. Breaking of abrasive-workpiece contact during grinding results in the formation of gaps between the cutting grits and workpiece surface [19]. This facilitates better penetration of the lubricant into the grinding zone, increasing the efficiency of lubrication. Hence when compared to all the other conditions employed, UAG + MQL has resulted in lowest value of grinding forces, as

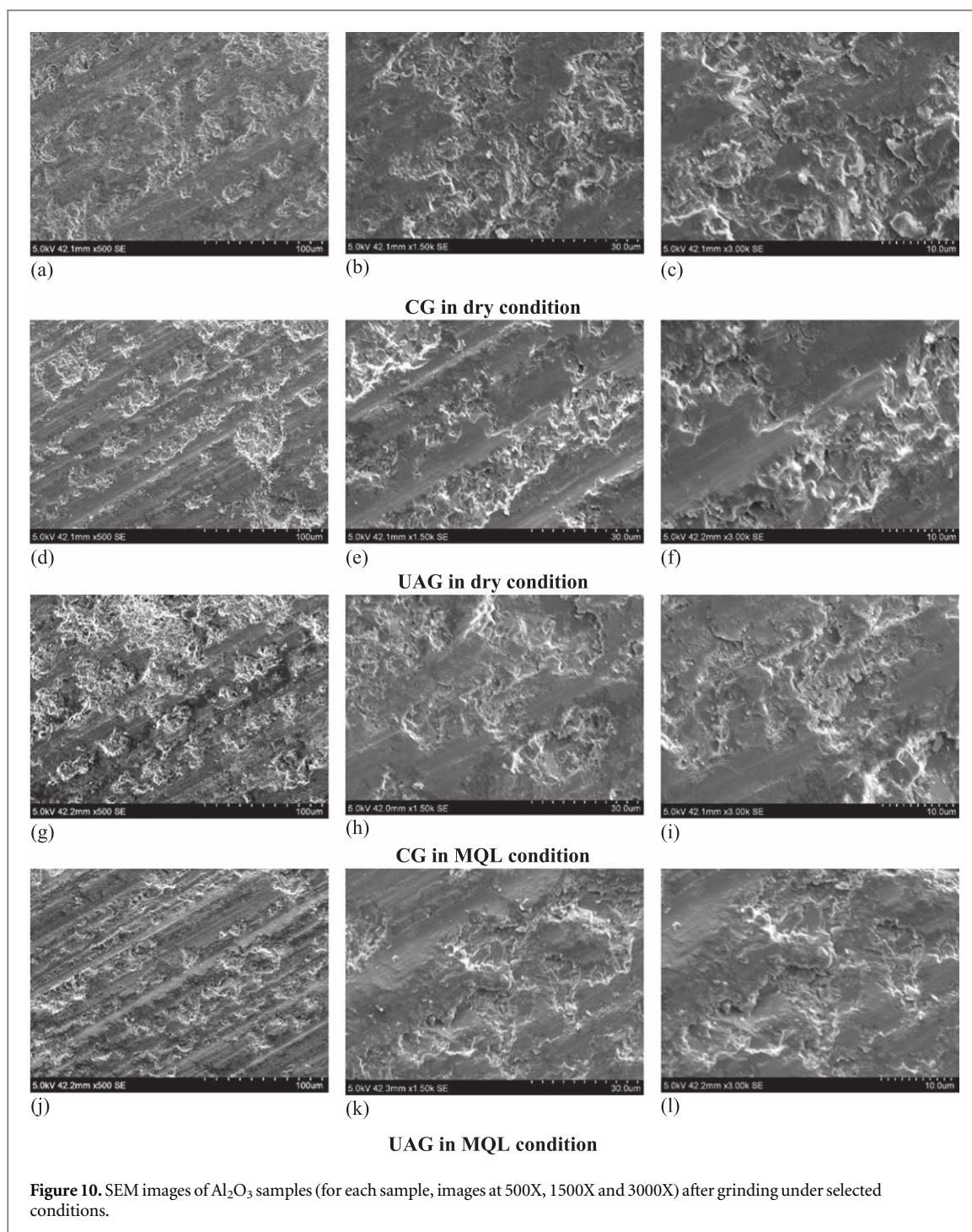


it combines the advantages of both techniques. The combination of MQL with UAG aids each other in lowering the forces while grinding.

#### 4.2. Analysis of 3D roughness parameters

Examination of 3D surface texture parameters can provide a proper insight into the quality of the ground surface. The parameters examined are  $S_a$  (arithmetic average roughness),  $S_q$  (RMS roughness),  $S_z$  (maximum peak to valley height) and  $S_p$  (height of largest peak). These parameters have been recommended for analysis of surface quality in ceramic samples machined using UAG by R Wdowik [40]. A comparative analysis of these parameters under different grinding conditions is done in figure 9. The roughness parameters are highest in the case of CG. The reduction of  $S_a$ ,  $S_q$ ,  $S_z$  and  $S_p$  values under UAG shows that the overall surface quality in terms of these parameters is enhanced by superimposing ultrasonic vibrations on to the workpiece. Kinematic simulations on the grinding traces of abrasives during UAG of ceramics performed by B Guo and Q Zhao [41] revealed that UAG has resulted in overlapping zones of grinding traces due to the imposed vibrations. The overlapping of abrasive traces translates into better surface finish in UAG. This effect is absent in CG, where the path traced by an abrasive on the workpiece surface is linear.

MQL grinding conditions record lower surface roughness values due to lower friction at the grinding zone which enables easier material removal. Emami *et al* [25] in their studies on grinding of alumina have obtained improved surface quality in MQL conditions. The same has been observed in the current experimental study. A decrease in normal forces in UAG facilitates better surface finish in grinding [19]. Hence UAG and MQL simultaneously work together in improving the surface quality. For instance, the area roughness parameter  $S_a$ ,



which was  $1.838 \mu\text{m}$  in CG is lowered to  $0.859 \mu\text{m}$  in UAG performed with MQL. A reduction of normal forces during UAG reduces the surface roughness. The presence of vibrations prevents the adhesion of chips on the newly formed surface, which improves the surface finish. While employing MQL during UAG, a better penetration of the lubricant to the grinding zone is expected [18]. Due to these factors, UAG performed in MQL condition has resulted in the minimum values for the surface roughness in terms of the parameters mentioned.

#### 4.3. Analysis of surface quality using SEM images and 3D profiles

The surface quality has been examined using SEM images. The SEM images of the surfaces obtained by grinding under dry and MQL conditions with and without ultrasonic assistance are shown in figures 10(a)–(l). The examination of SEM images shows that material removal mode while grinding of alumina is dominated by brittle fracture. Comparison of figures 10(a)–(c) with those at other grinding conditions shows that surface quality is worst in CG. While grinding brittle materials, material removal is through formation of the median-lateral crack system. The median cracks are formed by the penetration of the abrasive grits while grinding. These

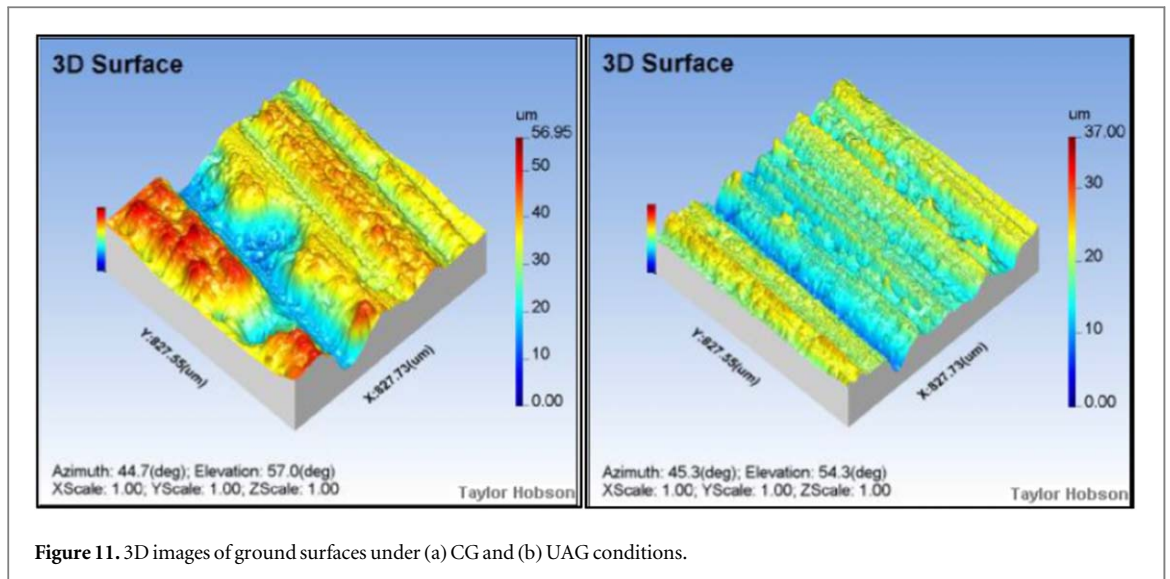


Figure 11. 3D images of ground surfaces under (a) CG and (b) UAG conditions.

cracks which extend vertically downward into the workpiece remain in the sub-surface even after grinding, resulting in reduction of strength. The formation and extension of lateral cracks parallel to the surface causes material removal by brittle fracture [42]. Hence it is essential to perform grinding of alumina under better grinding conditions by altering the process conditions. Even though grinding in MQL condition has improved the surface quality, it has still resulted in material removal by brittle fracture (figures 10(g)–(i)). However, from the analysis of SEM images in figures 10(d)–(f), it may be observed that there is a remarkable reduction in proportion of brittle fracture for samples processed by UAG compared to those in CG. This confirms the positive effect of inducing vibrations on to the workpiece while grinding. SEM images of workpieces obtained from grinding conditions where ultrasonic vibrations have been applied display visible ploughing marks, confirming that the proportion of material removed by ductile mechanism is higher in UAG. This is clearly apparent in the case of figures 10(j)–(l) which corresponds to the UAG + MQL condition.

Ductile removal of brittle material in CG is possible while grinding at depth of cut below a critical depth or at high cutting speeds. All depth of cuts employed in the current study are well above the critical depth of cut for alumina. Signs of ductile material removal have previously been observed by researchers while employing UAG for brittle materials [16]. Zhao *et al* [43] during grinding studies on nano-zirconia ceramics has observed that vibration assisted grinding results in a polishing effect, which increases the fraction of material removed by ductile mode and hence improves the ground surface quality. Analysis of the SEM images corresponding to vibration assisted grinding conditions, in both dry (figures 10(d)–(f)) and MQL (figures 10(j)–(l)) environments confirms the same. This is evident from the reduction of material removal by brittle fracture and the presence of ductile streaks on the surfaces generated by grinding in presence of vibration. Hence UAG promotes partial ductile mode grinding of brittle materials.

The 3D surface profile of the ground surfaces obtained using Talysurf CCI 3000 are shown in figures 11 and 12. The scanning area for the 3D scanner has been kept at  $1.8 \text{ mm} \times 1.8 \text{ mm}$ . All the other parameters for the non-contact profilometer were kept at their default values. The improvement in surface topography can be deduced from these 3D plots. The surface obtained by grinding in the MQL condition is better compared to that of CG. The surfaces generated in presence of ultrasonic vibration is more even, compared to the ones where vibrations were not provided. Analysis of the 3D surface profile parameters also confirm the enhancement of surface quality and the increase in proportion of ductile material removal. Kurtosis ( $S_{ku}$ ) value is a statistical measure of peaks present in the profiles of surfaces. Machined surface for which  $S_{ku} < 3$  is known as platykurtic, which denotes lesser distribution of sharp peaks on the surface. A surface whose  $S_{ku}$  is greater than 3 has a higher proportion of sharp peaks and is termed as leptokurtic. Hence  $S_{ku}$  can be used to measure flatness of the ground surface. The  $S_{ku}$  value obtained for conventional grinding is 2.375 and that of UAG is 4.432. The  $S_{ku}$  values for MQL and UAG + MQL are 2.406 and 3.423 respectively. This suggests that grinding with ultrasonic vibration assistance has resulted in the formation of surfaces dominated by sharp peaks. Choudhary *et al* [42] during their studies on grinding of alumina has elucidated the correlation between the nature of the surfaces generated in grinding and the mechanisms material removal. The nature of the surface formed after grinding is found to be dependent on the machining conditions. As it can be seen from figure 10(a), there is material removal in chunks caused by brittle fracture. This brittle fracture would have eliminated the peaks on the surface and hence resulted in lower kurtosis value in case of CG. The peaky surface in UAG is due to the reduction of brittle fracture and retention of grinding wheel profile on the ground surface. This is also applicable for grinding with and without

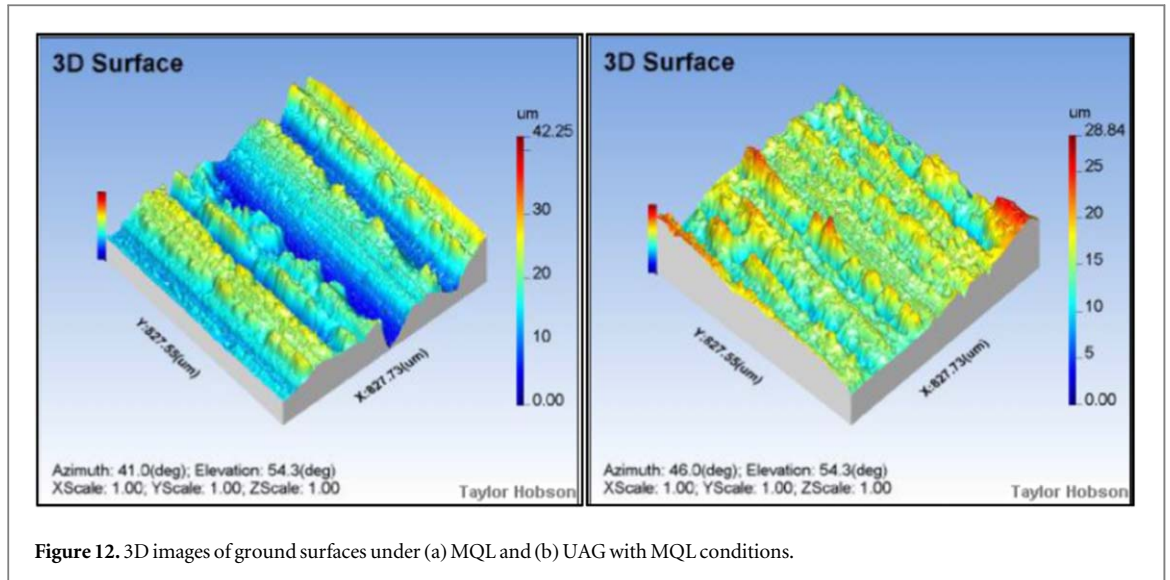


Figure 12. 3D images of ground surfaces under (a) MQL and (b) UAG with MQL conditions.

ultrasonic assistance in MQL condition. A higher kurtosis value is helpful for attaining improved load bearing ratio, better contact performance and higher lubrication retention [44]. Hence, examination of surface quality based on 3D roughness parameters and SEM images shows a significant improvement of surface topography.

The best surface quality has been obtained in the case of UAG in the presence of MQL, due to the combined effect of lubrication in MQL and polishing effect in UAG. The separation of abrasive-workpiece contact in UAG enabled the lubricant to penetrate efficiently into the grinding zone, thereby increasing the effectiveness of MQL.

## 5. Conclusion

The positive effects of providing the workpiece with ultrasonic vibrations have been confirmed by comparing the experimental data of CG and UAG. Optimisation of process parameters in UAG has been performed using combined Taguchi–GRA technique. The multiple response problem has been converted into optimisation of a single response characteristic which is the average GRG. The role of parametric optimisation in determining the appropriate combination of parameters to ensure optimal grinding characteristics has been established. Mathematical models developed using regression analysis could predict the experimental conditions with reasonable accuracy. A new set of grinding experiments have been conducted in dry and MQL conditions at the optimum set of UAG parameters. The findings from the experimental studies can be summarised as follows:

1. The selection of suitable parameter combination through optimisation is necessary for obtaining the beneficial effects of UAG. Multi-objective optimisation of UAG using GRA is found to be effective in identifying the optimum parameter combination that results in lowest grinding forces and surface roughness. ANOVA table for average GRG of multiple responses shows that the vibration amplitude and depth of cut has highest effect, followed by feed rate and wheel speed.
2. Contour plots for response variables suggest that better grinding characteristics are obtained while using higher values of vibration amplitude and wheel speed combined with lower values of feed rate and depth of cut.
3. The combination of highest amplitude and wheel speed levels with lowest feed rate and depth of cut has resulted in the optimum condition for multiple responses in UAG based on the average GRG. This corresponds to the condition  $A: -12 \mu\text{m}$ ,  $V_s: -30 \text{ m s}^{-1}$ ,  $V_w: -19 \text{ m min}^{-1}$  and  $a_e: -10 \mu\text{m}$ .
4. Grinding under UAG with MQL has combined the positive effects of both, resulting in the least grinding forces. Combining UAG with MQL has reduced the tangential force by 42% and normal force by 31% compared to CG.
5. Analysis of SEM images of the ground surface has shown that UAG has reduced the proportion of brittle fracture during grinding of alumina. Comparison of SEM images in CG and UAG shows the presence of ductile streaks on the ground surface. Hence it can be concluded that UAG promotes ductile mode of material removal in alumina. The improvement in quality of the ground surface has been established by examining 3D surface texture parameters. The surface quality based on roughness parameters  $S_a$ ,  $S_q$  and  $S_z$

has been compared for CG and UAG in dry and MQL conditions. The surface roughness in terms of these parameters are highest in CG. The highest surface quality in terms of the selected parameters and topographical features has been obtained by combining UAG with MQL. The surface roughness parameter  $S_a$ , has decreased from 1.838  $\mu\text{m}$  in CG to 0.859  $\mu\text{m}$  in UAG with MQL.

6. The selection of suitable parameter combination through optimisation is necessary for obtaining the beneficial effects of UAG. Multi-objective optimisation of UAG using GRA is found to be effective in identifying the optimum parameter combination that results in lowest grinding forces and surface roughness. ANOVA table for average GRG of multiple responses shows that the vibration amplitude and depth of cut has highest effect, followed by feed rate and wheel speed.
7. The analysis of kurtosis values for ground samples revealed that, surfaces generated by providing ultrasonic vibration assistance during grinding has resulted in generation of surfaces with  $S_{ku} > 3$ . This is characteristic of surfaces in which sharp peaks are prevalent. This is due to effective retention of grinding wheel profile on the ground surface which confirms the increase in material removal by ductile mode. Higher  $S_{ku}$  also indicates the generation of surfaces with better load bearing characteristics when compared to those samples ground without vibration assistance.
8. UAG has substantially reduced grinding forces and enhanced the surface quality. The combination of UAG with MQL has complemented their individual characteristics, resulting in an effective grinding process.

## Acknowledgments

The authors gratefully acknowledge Vellore Institute of Technology for providing access to the labs and instrumentation critical to this research work. This paper is part of an original research work carried out at Vellore Institute of Technology and has received no grants/financial support from any external agency.

## ORCID iDs

Sreethul Das  <https://orcid.org/0000-0002-8945-6228>

C Pandivelan  <https://orcid.org/0000-0001-8224-2959>

## References

- [1] Li K and Liao T W 1996 Surface/subsurface damage and the fracture strength of ground ceramics *Journal of Materials Processing Technology* **57** 207–20
- [2] Ding K, Fu Y, Su H, Xu H, Cui F and Li Q 2017 Experimental studies on matching performance of grinding and vibration parameters in ultrasonic assisted grinding of SiC ceramics *The International Journal of Advanced Manufacturing Technology* **88** 2527–35
- [3] Huang H and Liu Y C 2003 Experimental investigations of machining characteristics and removal mechanisms of advanced ceramics in high speed deep grinding *International Journal of Advanced Manufacturing Technology* **43** 811–23
- [4] Wang J, Zhang J, Feng P and Guo P 2018 Damage formation and suppression in rotary ultrasonic machining of hard and brittle materials: a critical review *Ceramics International* **44** 1227–39
- [5] Wan L, Liu Z, Deng Z, Li L and Liu W 2018 Simulation and experimental research on subsurface damage of silicon nitride grinding *Ceramics International* **44** 8290–6
- [6] Brehl D E and Dow T A 2008 Review of vibration-assisted machining *Precision Engineering* **32** 153–72
- [7] Xu W X and Zhang L C 2015 Ultrasonic vibration-assisted machining: principle, design and application *Advances in Manufacturing* **3** 173–92
- [8] O'Toole L, Kang C and Fang F 2019 Advances in rotary ultrasonic-assisted machining *Nanomanufacturing and Metrology* **3** 1–25
- [9] Dambatta Y S, Sarhan A A, Sayuti M and Hamdi M 2017 Ultrasonic assisted grinding of advanced materials for biomedical and aerospace applications—a review *The International Journal of Advanced Manufacturing Technology* **92** 3825–58
- [10] Kitzig-Frank H, Tawakoli T and Azarhoushang B 2017 Material removal mechanism in ultrasonic-assisted grinding of  $\text{Al}_2\text{O}_3$  by single-grain scratch test. *The International Journal of Advanced Manufacturing Technology* **91** 2949–62
- [11] Yang Z, Zhu L, Ni C and Ning J 2019 Investigation of surface topography formation mechanism based on abrasive-workpiece contact rate model in tangential ultrasonic vibration-assisted CBN grinding of  $\text{ZrO}_2$  ceramics *International Journal of Mechanical Sciences* **155** 66–82
- [12] Zhou W, Tang J and Shao W 2020 Modelling of surface texture and parameters matching considering the interaction of multiple rotation cycles in ultrasonic assisted grinding *International Journal of Mechanical Sciences* **166** 105246
- [13] Zheng K, Li Z, Liao W and Xiao X 2017 Friction and wear performance on ultrasonic vibration assisted grinding dental zirconia ceramics against natural tooth *Journal of the Brazilian Society of Mechanical Sciences and Engineering* **39** 833–43
- [14] Yang Z, Zhu L, Lin B, Zhang G, Ni C and Sui T 2019 The grinding force modeling and experimental study of  $\text{ZrO}_2$  ceramic materials in ultrasonic vibration assisted grinding *Ceramics International* **45** 8873–89
- [15] Kitzig-Frank H, Tawakoli T and Azarhoushang B 2017 Material removal mechanism in ultrasonic-assisted grinding of  $\text{Al}_2\text{O}_3$  by single-grain scratch test *The International Journal of Advanced Manufacturing Technology* **91** 2949–62
- [16] Li C, Zhang F, Meng B, Liu L and Rao X 2017 Material removal mechanism and grinding force modelling of ultrasonic vibration assisted grinding for SiC ceramics *Ceramics International* **43** 2981–93

- [17] Zheng W, Zhou M and Zhou L 2017 Influence of process parameters on surface topography in ultrasonic vibration-assisted end grinding of SiCp/Al composites *International Journal of Advanced Manufacturing Technology* **91** 2347–58
- [18] Molaie M M, Akbari J and Movahhedy M R 2016 Ultrasonic assisted grinding process with minimum quantity lubrication using oil-based nanofluids *Journal of Cleaner Production* **129** 212–22
- [19] Rabiei F A R S H A D, Rahimi A R and Hadad M 2017 Performance improvement of eco-friendly MQL technique by using hybrid nanofluid and ultrasonic-assisted grinding *International Journal of Advanced Manufacturing Technology* **93** 1001–15
- [20] Gao T, Zhang X, Li C, Zhang Y, Yang M, Jia D and Zhu L 2020 Surface morphology evaluation of multi-angle 2D ultrasonic vibration integrated with nanofluid minimum quantity lubrication grinding *Journal of Manufacturing Processes* **51** 44–61
- [21] Mandal N, Doloi B, Mondal B and Das R 2011 Optimization of flank wear using zirconia toughened alumina (ZTA) cutting tool: Taguchi method and regression analysis *Measurement* **44** 2149–55
- [22] Chang C W and Kuo C P 2007 Evaluation of surface roughness in laser-assisted machining of aluminum oxide ceramics with Taguchi method *International Journal of Machine Tools and Manufacture* **47** 141–7
- [23] Joel J and Xavier A 2019 Optimization on machining parameters of aluminium alloy hybrid composite using carbide insert *Materials Research Express* **6** 116532
- [24] Fratila D and Caizar C 2011 Application of Taguchi method to selection of optimal lubrication and cutting conditions in face milling of AlMg<sub>2</sub> *Journal of Cleaner Production* **19** 640–5
- [25] Emami M, Sadeghi M H, Sarhan A A D and Hasani F 2014 Investigating the Minimum Quantity Lubrication in grinding of Al<sub>2</sub>O<sub>3</sub> engineering ceramic *Journal of Cleaner Production* **66** 632–43
- [26] Julong D 1989 Introduction to grey system theory *The Journal of Grey System* **1** 1–24 (<https://pdfs.semanticscholar.org/3d6b/22f0a4611319a424235c7516eb5352645616.pdf>)
- [27] Sarkaya M and Gullu A 2015 Multi-response optimization of minimum quantity lubrication parameters using Taguchi-based grey relational analysis in turning of difficult-to-cut alloy Haynes 25 *Journal of Cleaner Production* **91** 347–57
- [28] Maiyar L M, Ramanujam R, Venkatesan K and Jerald J 2013 Optimization of machining parameters for end milling of Inconel 718 super alloy using Taguchi based grey relational analysis *Procedia Engineering* **64** 1276–82
- [29] Rajyalakshmi G and Ramaiah P V 2013 Multiple process parameter optimization of wire electrical discharge machining on Inconel 825 using Taguchi grey relational analysis *The International Journal of Advanced Manufacturing Technology* **69** 1249–62
- [30] Selvakumar V, Muruganandam S, Tamizharasan T and Senthilkumar N 2016 Machinability evaluation of Al–4% Cu–7.5% SiC metal matrix composite by Taguchi–Grey relational analysis and NSGA-II *Sadhana* **41** 1219–34
- [31] Wdowik R, Porzycki J and Magdziak M 2017 Measurements of surface texture parameters after ultrasonic assisted and conventional grinding of ZrO<sub>2</sub> based ceramic material characterized by different states of sintering *Procedia CIRP* **62** 293–8
- [32] Zhong Z, Ramesh K and Yeo S H 2001 Grinding of nickel-based super-alloys and advanced ceramics *Materials and Manufacturing Processes* **16** 195–207
- [33] Malkin S and Hwang T W 1996 Grinding mechanisms for ceramics *CIRP Annals* **45** 569–80
- [34] Ostasevicius V, Jurenas V, Balevicius G and Cesnavicius R 2020 Development of actuators for ultrasonically assisted grinding of hard brittle materials *The International Journal of Advanced Manufacturing Technology* **106** 289–301
- [35] Baraheni M and Amini S 2019 Predicting subsurface damage in silicon nitride ceramics subjected to rotary ultrasonic assisted face grinding *Ceramics International* **45** 10086–96
- [36] Wang Y, Guangheng D, Zhao J, Dong Y, Zhang X, Jiang X and Lin B 2019 Study on key factors influencing the surface generation in rotary ultrasonic grinding for hard and brittle materials *Journal of Manufacturing Processes* **38** 549–55
- [37] Emami M, Sadeghi M H and Sarhan A A 2013 Investigating the effects of liquid atomization and delivery parameters of minimum quantity lubrication on the grinding process of Al<sub>2</sub>O<sub>3</sub> engineering ceramics *Journal of Manufacturing Processes* **15** 374–88
- [38] Baraheni M and Amini S 2019 Investigation on rotary ultrasonic assisted end grinding of silicon nitride ceramics *SN Applied Sciences* **1** 1560
- [39] Ibrahim E E, Checkley M, Chen X, Sharp M, Liang W, Yuan S and Batako A D L 2019 Process performance of low frequency vibratory grinding of inconel 718 *Procedia Manufacturing* **30** 530–5
- [40] Wdowik R 2018 Measurements of surface texture parameters after ultrasonic assisted and conventional grinding of carbide and ceramic samples in selected machining conditions *Procedia CIRP* **78** 329–34
- [41] Guo B and Zhao Q 2017 Ultrasonic vibration assisted grinding of hard and brittle linear micro-structured surfaces *Precision Engineering* **48** 98–106
- [42] Choudhary A, Naskar A and Paul S 2018 Effect of minimum quantity lubrication on surface integrity in high-speed grinding of sintered alumina using single layer diamond grinding wheel *Ceramics International* **44** 17013–21
- [43] Zhao B, Chang B, Wang X and Bie W 2019 System design and experimental research on ultrasonic assisted elliptical vibration grinding of Nano-ZrO<sub>2</sub> ceramics *Ceramics International* **45** 24865–77
- [44] Wang W Z, Chen H, Hu Y Z and Wang H 2006 Effect of surface roughness parameters on mixed lubrication characteristics *Tribology International* **39** 522–7